PCCP

Accepted Manuscript

ROYAL SOCIETY OF CHEMISTRY

www.rsc.org/pccp

Journal Name

RSCPublishing

ARTICLE

Scalable production of winkled and few-layered graphene sheets and their use for oil and organic solvents absorption

Cite this: DOI: 10.1039/x0xx00000x

Dan Liu, Weiwei Lei,* and Ying Chen*

Received 00th January 2012,
Accepted 00th January 2012

DOI: 10.1039/x0xx00000x

www.rsc.org/

High-quality winkled and few-layered graphene sheets have been produced via a mechano-thermal exfoliation process for a simple, effective and low-cost mass production in which the graphene sheets were produced by first ball milling of graphite with ammonium chloride and followed by a thermal annealing at 800 °C in nitrogen gas. The few layered graphene sheets show highly efficient selectivity and capacity for the absorption of from petroleum products to organic solvents such as ethanol, cyclohexane and chloroform (up to 82, 42 and 98 times of its own weight, respectively). The saturated few-layered graphene sheets can be cleaned for reuse by simply burning in air. The low-cost strategy for mass production and easy recycling routes demonstrate the great potential of few-layered graphene sheets for oil removal.

Introduction

Graphene is a single atom-thick sheet of graphite and arranged in a tightly packed into a honeycomb two-dimensional (2D) lattice. Since the discovery in 2004,[1] it has rapidly become popular because of its distinctive physical and chemical properties and potential applications in flexible electronics,[2] transparent conductive electrodes,[3] nanoscale electronic deviceds,[4] energy research and catalysis,[5] and composite materials.[6] To date, many chemical approaches have been developed for the synthesis of graphene, including chemical or thermal reduction of graphene oxide (GO),[7] chemical vapour deposition (CVD)[8], epitaxial growth[9] and organic solvent dispersion method.[10] Despite of large-scale production of graphene materials have been realized through chemical methods, these processes are labor intensive and involve strong corrosive, volatile, or hazardous oxidizing reagents.[11]Exfoliation method is another good option for prodiucing graphene sheets with high structure quality. Han et al. reported that monolayer graphene can be obtained through a mechanical exfoliation method. Although the sheets have very high quality but production yield is very low.[12] Recently, liquid-phase exfoliation of natural graphite has opened up a simple way to prepare graphene simply using sonication of graphite powders in various solvents (such as N-methyl-pyrrolidone and 1,2-dichlorobenzene) or surfactants solutions.[13,14] However, these methods have some fatal disadvantages: the amount of exfoliated product is usually very low and limited relatively to the starting material; excessive sonication and centrifugation treatment can damage the graphene structure; the dispersed graphene easily tend to aggregate during drying process. On the other hand, ball milling method has been envisaged to handle these problems but usually results in poor purity and a mixture of a wide variety of graphitic materials: single- and multi-layer graphene and un-exfoliated graphite.[15-20] Thus, the development of new facile and solid-phase approaches for high-yield production of high quality graphene is highly desired.

Herein we report a new exfoliation route for a simple, effective and large scale production of few layered graphene sheets. This technique is based on solid-exfoliation of graphite using ball milling method to obtain high quality winkled and good selectivity toward few-layered graphene sheets without involving any catalyst, template or solvent. The difference in terms of selectivity versus previously reported routs may originate from the use of a specific reactant (ammonium chloride) that could intercalate efficiently between the graphite sheets and strongly improve the exfoliation process. The few-layered graphene sheets show excellent sorption performances for a wide range of oils and organic solvents, with mass uptakes reaching 98 × its own weight, due to a combination of high winkle, 2D structure and porosity. In addition, the saturated material can be cleaned by simply burning or heating for recycling use.

Results and discussion

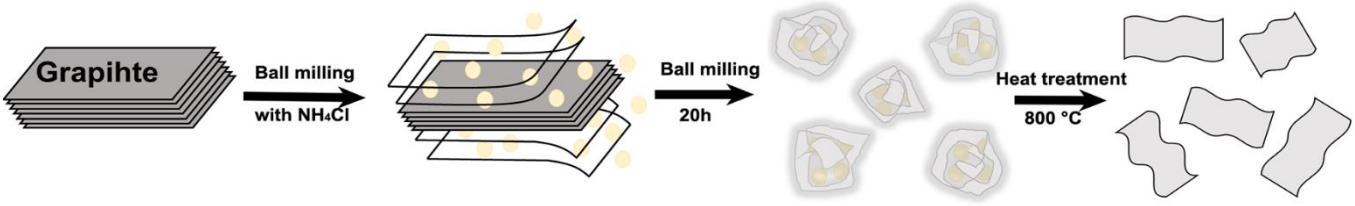

Figure 1. Schematic of the synthetic process that involves milling of graphite with NH_4Cl particles to form graphene-wrapped NH_4Cl particles, followed by heating at 800 °C to achieve few-layered graphene sheets.

The new exfoliation procedure is presented in **Fig. 1**. This exfoliation process involves three stages: 1) the milling balls inside of the milling cells rotating at a high speed of 700 rpm of generate sufficient kinetic energy to overcome the van der Waals interactions between adjacent graphite layers, and produce a large number of nanosheets at the end of 5h of milling. 2) further milling leads to fully graphene-wrapped NH_4Cl particles. 3) thermal pyrolytic process of the milled composite powder at 800 °C under flowing N_2 for 1h produces winkled and few-layered graphene sheets as final product. Importantly, the final graphene produced has a very high yield closed to the amount of graphite precursor.

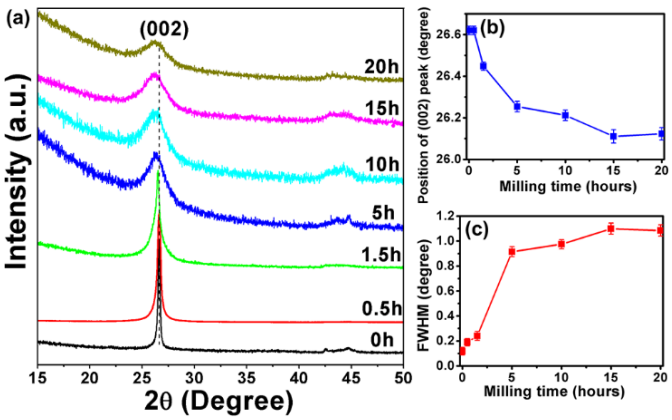

Figure 2. (a) Representative XRD patterns of graphite with different milling periods. The milling time dependence of (b) position and (c) FWHMs of (002) diffraction peaks.

The XRD patterns of graphite for different milling periods after heating are displayed in **Fig. 2a**. The pristine graphite shows a characteristic peak centred at 2θ = 26.6°, belonging to the (002) interlayer reflection of graphite with a *d* value of 3.351Å. The 2θ position of (002) peak gradually shifts to the low degree with the increase of ball milling time to 20h, as shown in **Fig. 2b**. The lamellar stacking distance of graphite after 20h milling was estimated to be 3.41Å on the basis of the very broad (002) peak centered at 26.12 °, suggesting that the gradual exfoliation process from graphite to graphene sheets. The XRD patterns show systematic changes in the full width at half-maximum (FWHM) of (002) peak as a function of the milling time (**Fig. 2c**). A significant increase of the FWHM of (002) peak from 0.118 ° to 0.915 ° is observed during the first 5h of milling and then slowly increases to 1.085 ° during extended milling to 15h. The FWHM of the (002) peak does not change much during further milling to 20h. The increase of FWHM indicates the reduced graphite thickness, which agree well with TEM and AFM images.

Raman spectroscopy is an efficient non-destructive method to characterize the thickness and quality of as- prepared graphene. Representative Raman spectra of bulk graphite and graphene sheets under different milling times in the frequency range of 1200-3300 cm^{-1} are shown in **Fig. 3**. Three prominent bands can be seen in the spectrum of the pristine graphite, which are assigned to D, G, and 2D bands, at the positions of around 1350, 1582, and 2718 cm^{-1}, respectively.[21] The D band is attributed to the breathing modes of sp^2 rings and requires a defect for its activation i.e., vacancies, or grain boundaries/edges.[22] The G peak corresponds to the optical E_{2g} phonon at the Brillouin zone center. With increasing of the milling time, there is a new Raman peak appears as a shoulder around 1630 cm^{-1} on the G band, named D' band. The high relative intensity of D and D' bands in the spectra after milled 1.5h indicate that the formation of graphene after synthesis and a large amount of defects in graphene induced by high-energy ball milling.[23,24] In addition, the shape of 2D band and the intensity ratio of I_{2D}/I_G, are widely used to identify size of graphene sheets. The intensity ratio of I_{2D}/I_G increases from 0.26 to 0.61 with increasing the milling time to 20h, as shown in **Fig. 3**, indicating the reduced graphite thickness.

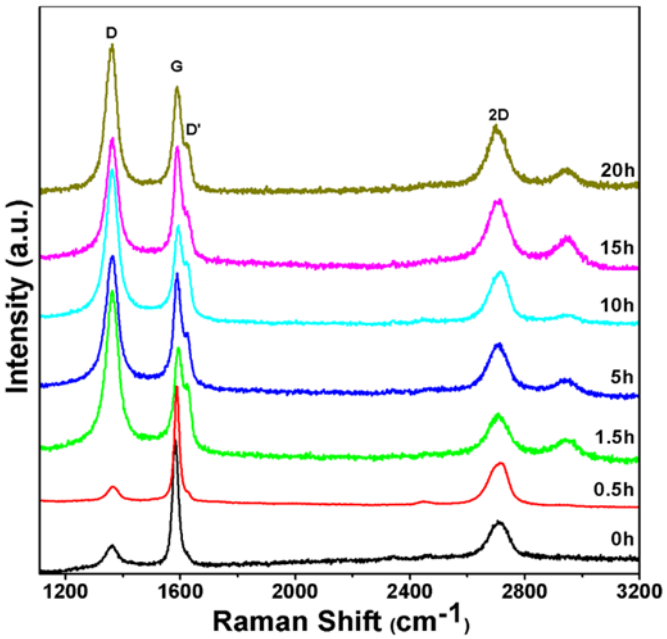

Figure 3. Raman spectra of the graphite milled for different periods and heating at 800 °C using a 514.5 nm line of an argon ion laser.

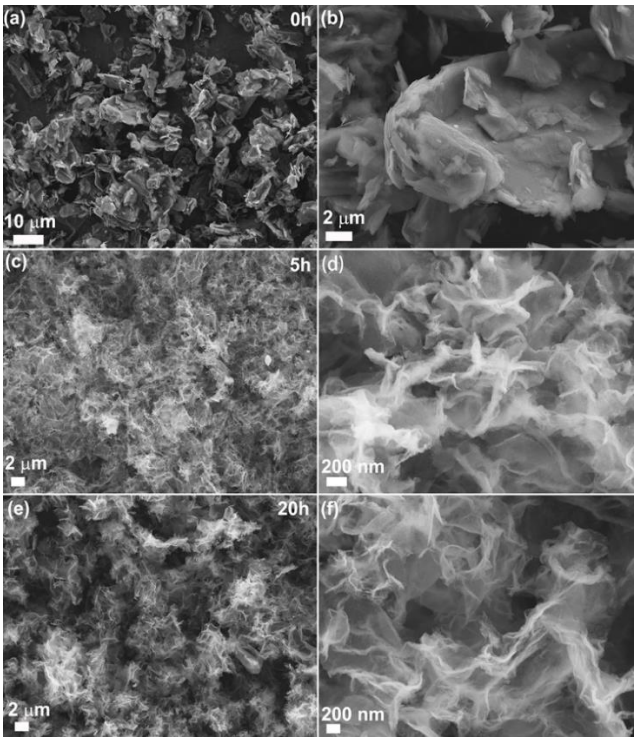

Figure 4. SEM images and the corresponding magnification of (a,b) pristine graphite, (c,d) milled for 5h after heating and (e,f) millled for 20h and heating at 800 °C.

Representative scanning electron microscopy (SEM) images of as-obtained samples are shown in **Fig. 4**. The pristine graphite samples

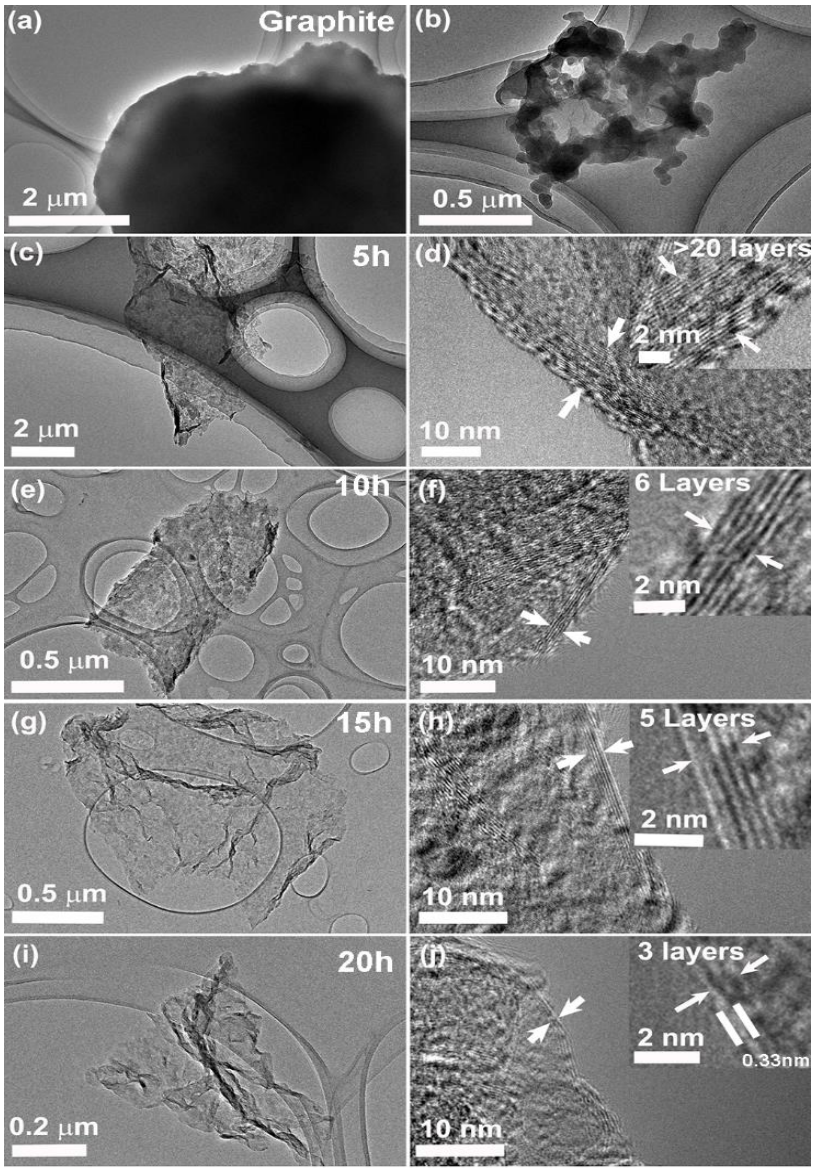

Figure 5. TEM images of pristine graphite (a,b), and TEM and HRTEM images of graphite milled for (c,d) 5h, (e,f) 10h, (g,h) 15h, and (i,j) 20h and heating at 800 ºC. The insets show the number of layers highlighted by white arrows.

show many aggregation of thick flakes (**in Fig. 4a**). Compared with the initial graphite, the sizes and thickness of graphite were obviously reduced after ball milling for 5h and heating, as shown in **Fig. 4b**. The fluffy and crumpled of free-standing few layered graphene are observed with continuously milling to 20h after heating (**in Fig. 4c,d**). The detailed morphologies and structures of the samples were further studied by transmission electron microscopy (TEM) and high-resolution TEM (HRTEM). Compared to the initial graphite (Figure 5a, b), it is clearly observed that the exfoliated graphene sheets became wrinkles and almost transparent under the electron beam suggesting the formation of ultrathin graphene sheets after ball milling 5-20h and heating at 800 ºC, as shown in Figure 5c, e, g, and i. The detailed thickness of the exfoliated graphene sheets can be obtained by examining the edges from their correspondence HRTEM images **Fig. 5d, f, h, and j**. It can be seen clearly that more than 20, 6, 5 and 3 parallel fringes corresponding to more than 20, 6, 5 and 3 stacked layers in the exfoliated samples after ball milling for 5, 10, 15 and 20h and annealing at 800 ºC, respectively, indicating the thickness of exfoliated graphene sheets gradually decrease with the increase of ball milling time.

Atomic force microscopy (AFM) was then employed to further analyse the thickness and fine structure of the graphene sheets. The AFM images of graphene sheet obtained from graphite after 20h milling and heating (in **Fig. 6d**) directly prove the presence of a layer structure of sheets on a mica substrate with a uniform layer thickness of about 0.8 nm. Thus, the number of layers deduced from the AFM data is less than three, which is in good agreement with the HRTEM observation (**Fig. 5f**). In addition, a series of graphene sheets produced with different milling time were studied. As shown in **Fig. 6**, the topographic heights are around 6.9, 2.4, 1.6, and 1.0 nm, for milling time of 5, 10, 15, and 20h, respectively. This indicates that the heights distribution of the graphene layers is from 22 to 3 layers. Therefore, both HRTEM and AFM results reveal the exfoliation process as a

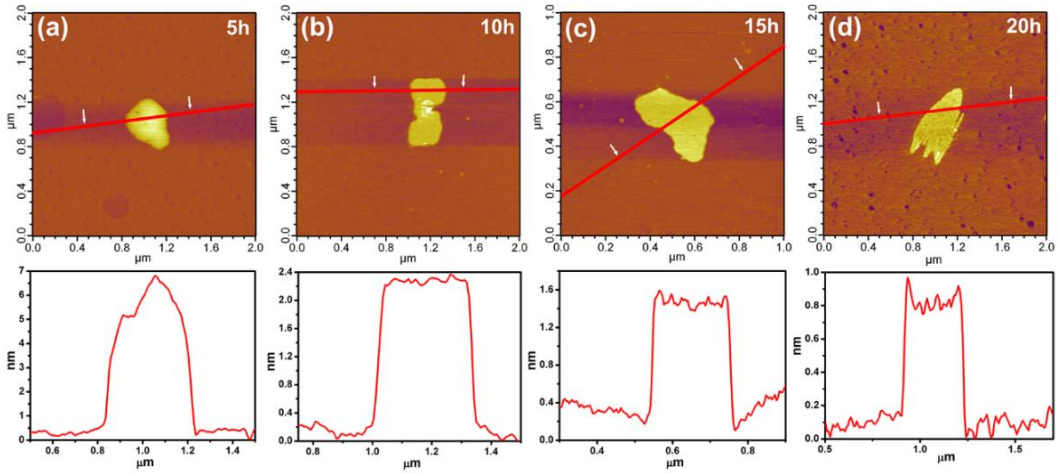

Figure 6. High-magnification AFM image of graphite milled for different periods and heating at 800 °C. The height profiles showing typical size and thickness of a single graphene.

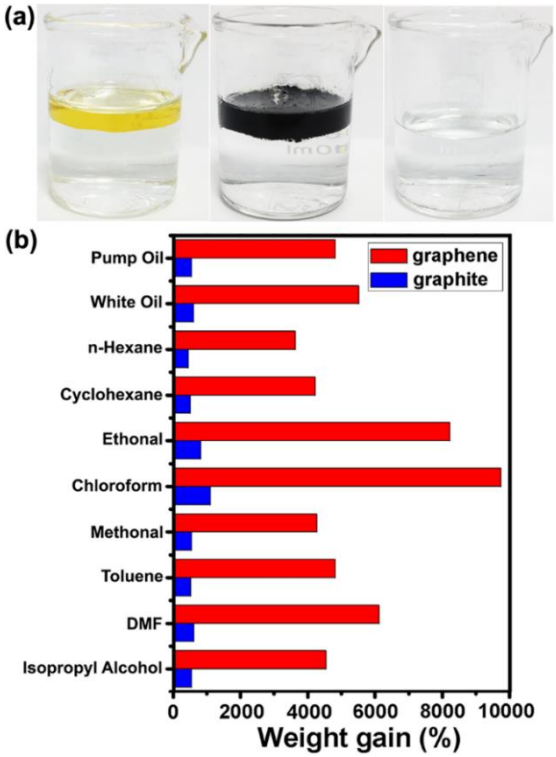

Figure 7. Absorption tests for few-layered graphene sheets. (a) Oil removal from water surface. Left: 3.5 mL pump oil floating on the surface of 20 mL water in a beaker. Middle: 15 mg of the few-layered graphene sheets of milled 20h are added. The graphene powders disperse selectively in the oil layer, while the water remains clear. Right: removal of the graphene–oil slurry by filtration, while the water remains clear. (b) Absorption capacities for different organic liquids measured by direct weighing for graphite and few-layered graphene sheets.

function with the increasing of the ball milling time, indicating the thickness of graphene sheets can be controlled by ball milling time.

Oil spillages and organic solvents discharged from industries are primary pollutants of water resources. A number of advanced nanomaterials[25-27] has been processed and showed excellent

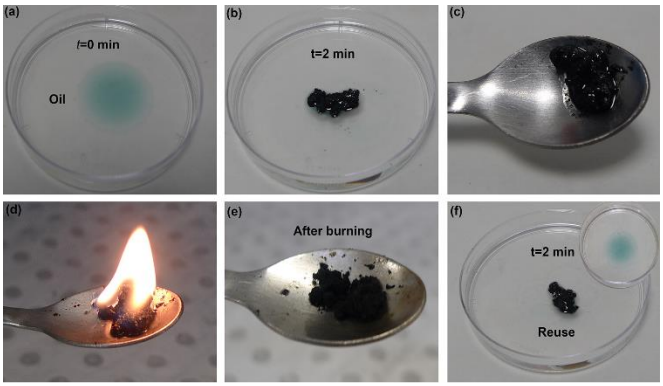

Figure 8. Photograph of dyed oil for oil absorption tests with few-layed graphene. (b) Photograph of few-layed garaphene saturated with oil after 2 min of absorption. (c) Photograph of collecting oil-saturated graphene. (d) Photograph of burning oil-saturated graphene in air for cleaning purpose. (e) Photograph of prepred graphene after burning. (f) Photograph of the cleaned graphene for second oil absorption test after 2 min, the insert shows the dyed oil for retest.

absorption behaviours. Few-layered graphene sheets (after milling 20h and heating at 800 °C) exhibits excellent absorbencies for oils and organic solvents. The evolvement of absorbing the pump oil is shown in a series of photos in **Fig. 7a**. When the black graphene sheets meet with yellow pump oil, the oil is absorbed immediately by the sheets. The saturated sheets still float on clean water surface, which makes them easy to be collected. In addition, the absorption of several classes of organic solvents was evaluated in this study and the results are shown in **Fig.7b**. The efficiency of absorption can be referred to as weight gain (wt%) defined as the weight of absorbed substances per unit weight of graphene sheets. The absorption capability of as-obtained few-layered graphene sheets was generally >50× its own weight. For instance, the absorption toward white oil, ethanol and chloroform is close to 55×, 82× and 98×, respectively, which is much higher than pristine graphite as well as common absorbents and other recently-reported nanomaterials and macrostructures, i.e. collagen nanocomposites,[28] polyurethane and iron oxide composites,[29]graphene hydrogels,[30] and MnO_2 nanowires[31]. Importantly, the absorbed oil or solvents could be removed from the

thermally-stable graphene sorbent by direct combustion in air for reuse in **Fig. 8**. The high absorption capacity of the few-layered graphene sheets for oils and organic solvents is essentially due to their large surface area 315 m^2/g (**Fig. S1**), two dimensional which exacerbate interfacial interactions.[25,32] The few-layered graphene sheets (several micrometers wide and few nanometers thick) have a large number of edges with unsaturated atoms after ball milling, which are chemically more reactive than perfect graphite basal planes, and act as absorption sites for organic molecules. Capillary forces also act in the porous structure to increase the absorption capacity compared to bulk graphite powders.[31]

Conclusions

In summary, highly winkled and few-layered graphene sheets have been synthesized using a ball milling process without the use of any catalysis and ex situ template. The obtained few-layered graphene sheets show high selective absorption and adsorption capacities for oils and organic solvents. These winkled and few-layered graphene sheets can be reused for environmental remediation through regeneration upon burning in air. All these features make these few-layered graphene sheets suitable for a wide range of applications in water cleaning.

Experimental

Materials synthesis. In a typical synthesis experiment, graphite and ammonium chloride (NH_4Cl) powders with the mole ratios of 1:14 were loaded inside a steel milling container (Pulverisette 7, Fritsch). The powder mixture was milled at a rotation speed of 700 rpm for different times up to 20h at room temperature under nitrogen atmosphere of 100 kPa. After ball milling, the mixture powders were loaded into a quartz boat and then heated at a rate of 10 ℃/min and kept at 800 ℃ for 1 h under a nitrogen gas flow. During the heating treatment, the NH_4Cl was decomposed to various gases and the releasing gas bubbles left porous structure in final product. The NH4Cl acted as fugitive templates resulting

Materials characterization. The crystallite structures were determined by X-ray powder diffraction (XRD) (Panalytical X'Pert PRO system) using Cu Kα radiation. Raman measurement was investigated using Renishaw Raman spectrometer with a laser wavelength of 532 nm at room temperature. To avoid the inhomogeneous distribution in samples, Raman spectra were collected at three different dots for each sample. The morphologies of the samples were characterized using a field emission scanning electron microscope (SEM, Zeiss Supra 55 VP) and transmission electron microscopy (TEM, JEOL 2100F) in high resolution mode operating at 110kV. The AFM measurements were performed on a Cypher atomic force microscope.

Acknowledgements

Financial support from the Australian Research Council under the Discovery Project and DECRA Research Fellowship, and Central Research Grant Scheme (CRGS) from Deakin University are acknowledged. All Raman experiments conducted here were undertaken on the combined FTIR/Raman microspectroscopic instrument funded by the ARC-LIEF grant (Project ID. LE120100166)

Author Information

Corresponding Authors: weiwei.lei@deakin.edu.au; ian.chen@deakin.edu.au

Notes and references

Institute for Frontier Materials
Deakin University, Waurn Ponds, Victoria 3216, Australia

1. K. S. Novoselov, A. K. Gleam, S. V. Morozov, D. Jiang, Y. Zhang, S. V. Dubonos, I. V. Grigorieva, and A. A. Firsov, *Science*, 2004, **306**, 666.
2. K. S. Kim, Y. Zhao, H. Jang, S. Y. Lee, J. M. Kim, K. S. Kim, J. H. Ahn, P. Kim, J. Y. Choi, and B. H. Hong, *Nature*, 2009, **457**, 706.
3. X. Li, Y. Zhu, W. Cai, M. Borysiak, B. Han, D. Chen, R. D. Piner, L. Colombo, *and* R. S. Ruoff, *Nano Lett.* 2009, **9**, 4359.
4. Y. W. Son, M. L. Cohen, and S. G. Louie, *Nature*, 2006, **444**, 347.
5. H. Wang, Y. Liang, T. Mirfakhrai, Z. Chen, H. S. Casalongue and H. Dai, *Nano Res.*, 2011, **4**, 729.
6. Q. Wu, Y. Xu, Z. Yao, A. Liu, and G. Shi, *ACS Nano*, 2010, **4**, 1963.
7. S. Niyogi, E. Bekyarova, M. E. Itkis, J. L. Mcwilliams, M. A. Hamon, and R. C. Haddon, *J. Am. Chem. Soc.* 2006, **128**, 7720.
8. H. Shu, X. Chen, X. Tao, and F. Ding, *ACS Nano*, 2012, **6,** 3243.
9. P. W. Sutter, J. -I. Flege, and E. A. Sutter, *Nat. Mater.* 2008, **7**, 406.
10. X. Zhang, A. C. Coleman, N. Katsonis, W. R. Browne, B.J. van Wees, and B. L. Feringa, *Chem. Commun*, 2010, **46**, 7539.
11. D. Li, M. B. Müller, S. Gilje, R. B. Kaner, and G. G. Wallace, *Nature Nanotechnology*, 2008, **3**, 101.
12. M. Y. Han, B. Özyilmaz, Y. Zhang, and P. Kim, *Phys. Rev. Lett.* 2007, **98**, 206805.
13. Y. Hernandez, V. Nicolosi, M. Lotya, F. M. Blighe, Z. Sun, S. De, I. T. Mcgovern, B. Holland, M. Byrne, Y. k. Gun'ko, J. J. Boland, P. Niraj, G. Duesberg, S. Krishnamurthy, R. Goodhue, J. Hutchison, V. Scardaci, A. C. Ferrari and J. N. Coleman, *Nat. Nanotechnol.*, 2008, **3**, 563.
14. M. Lotya, Y. Hernandez, P. J. King, R. J. Smith, V. Nicolosi, L. S. Karlsson, F. M. Blighe, S. De, Z. M. Wang, I. T. McGovern, G. S. Duesberg and J. N. Coleman, *J. Am. Chem. Soc.*, 2009, **131**, 3611.
15. R. Aparna, N. Sivakumar, A. Balakrishnan, A. S. Nair, S. V. Nair, and K. R. V. Subramanian, *J. Renew. Sustain. Energy*, 2013, **5**, 033123.
16. A. E. D. Rio-Castillo, C. Merino, E. Diez-Barra and E. Vazquez, *Nano Research*, 2014, **7**, 963.
17. M. Mao, S. Z. Chen, P. He, H. L. Zhang and H. T. Liu, *J. Mater. Chem. A*, 2014, **2**, 4132.
18. V. Leon, A. M. Rodriguez, P. Prieto, M. Prato and E. Vazquez, *ACS Nano*, 2014, **8**, 563.
19. I. Y. Jeon, Y. R. Shin, G. J. Sohn, H. J. Choi, S. Y. Bae, J. Mahmood, S. M. Jung, J. M. Seo, M. J. Kim, D. W. Chang, L. M. Dai and J. B. Baek, *PNAS*, 2012, **109**, 5588.
20. I. Y. Jeon, H. J. Choi, M. J. Ju, I. T. Choi, K. Lim, J. Ko, H. K. Kim, J. C. Kim, J. J. Lee, D. Shin, S. M. Jung, J. M. Seo, M. J. Kim, N. Park, L. M. Dai and J. B. Baek, *Scientific reports*, 2013, **3**, 2260.
21. T. Xing, L. H. Li, L. T. Hou, X. P. Hu, S. X. Zhou, R. Peter, M. Petravic, Y. Chen, *Carbon*, 2013, **57**, 515.
22. L. M. Malard, M. A. Pimenta, G. Dresselhaus, M. S. Dresselhaus, *Phys. Rep.* 2009, **473**, 51.
23. H. B. Wang, C. Zhang, Z. H. Liu, L. Wang, P. X. Han, H. X. Xu, K. J. Zhang, S. M. Dong, J. H. Yao, and G. L. Cui, *J. Mater. Chem.*, 2011, **21**, 5430.
24. D. Liu, W. W. Lei, D. Portehault, S.Qin and Y. Chen, *J. Mater. Chem. A*, 2015, **3**, 1682.
25. W. W. Lei, D. Portehault, D. Liu, S.Qin, and Y. Chen. *Nature Comm* 2013, **4**, 1777.
26. K. Sohn, Y. J. Na, H. Chang, K. M. Rob, H. D. Jang, and J. X. Huang, *Chem. Commun.* 2012, **48**, 5968.
27. Q. Zhu, Q. M. Pan, F. T. Liu, *J. Phys. Chem. C*, 2011, **115**, 17464.
28. P. Thanikaivelan, N. T. Narayanan, B. K. Pradhan, and P. M. Ajayan, *Sci. Rep*. 2012, **2**, 230.
29. P. Calcagnile, D. Fragouli, I. S. Bayer, G. C. Anyfantis, L. Martiradonna. P. D. Cozzoli, R. Cingolani, and A. Athanassiou, *ACS Nano.* 2012, **6**, 5413.

30. H. P. Cong, X. C. Ren, P. Wang, and S. H. Yu, *ACS Nano.* 2012, **6**, 2693.
31. J. K. Yuan, X. G. Liu, O, Akbulut, J. Q. Hu, S. L. Suib, J. Kong, F. Stellacci, *Nat. Nanotechnol.* 2008, **3**, 332.
32. D. Liu, W. W. Lei, S. Qin, and Y. Chen，*Sci. Rep*. 2014, **4**, 4453.

